Mineral. Soc. Amer. Spec. Pap. **3,** 113–121 (1970).

CREEP IN THE UPPER MANTLE[1]

C. Barry Raleigh and Stephen H. Kirby
U.S. Geological Survey, Menlo Park, California

Abstract

Creep experiments on lherzolite and dunites at high temperature, 0.6 to 0.7 T_m, and confining pressure show that the strain rate, $\dot{\epsilon}$, is given by

$$\dot{\epsilon} = A\sigma^5 \exp \frac{-Q_c}{RT}$$

where σ is the stress difference and Q_c, the activation energy. Assuming the activation energy for creep is equal to the activation energy for self-diffusion permits extrapolation of this flow equation and theoretical creep equations to mantle conditions. The results show a strong dependence on the mantle temperature. For low assumed temperatures the upper mantle has an effective viscosity of 5×10^{21} poises at $\dot{\epsilon}=10^{-14}$ sec^{-1}, and creeps according to the experimentally derived power law equation. If the temperatures are assumed to be higher, the viscosities are lower and Herring-Nabarro creep dominates. Evidence from microstructures indicates that olivine in the region of the mantle from which ultramafic xenoliths are derived has been deformed by the same creep processes as occur in the laboratory experiments. Therefore, at least in the uppermost mantle, power-law creep has been important.

Introduction

The creep strength of the mantle is of considerable interest now that large, approximately steady-state mantle deformations associated with sea-floor spreading have been demonstrated. In earlier discussions of this subject (Gordon, 1965, 1967; McKenzie, 1968; Weertman, 1970), the strength of the mantle was analyzed by applying one or another of several theoretical models of the creep process to rocks under mantle conditions. The results were qualitatively valuable but of questionable quantitative validity, inasmuch as no direct empirical data on creep of rocks of probable mantle composition were available. Until recently, apparatus in which creep experiments could be conducted under upper-mantle conditions was not available. Development of such apparatus by D. T. Griggs and his co-workers has enabled study of creep of polycrystalline olivine in several laboratories; reanalysis of creep in the mantle is therefore in order. In this paper we will follow Weertman's (1970) analysis and substitute empirically determined parameters, where applicable, into Weertman's equations.

Other than by measuring the time dependence of the response of the earth to changes in load, the only way to test models of the creep behavior of the mantle is by examining the microstructure of xenoliths brought up from the mantle by volcanism. Assuming that the same creep process will produce the same microstructures regardless of strain rate or temperature, comparison between experimental and natural microstructures should serve to identify the creep process in the upper mantle. These comparisons are made in this paper and, in addition, a method for estimating stresses in the mantle from the comparison is described.

[1] Publication authorized by the Director, U. S. Geological Survey. An independent analysis of the viscosity of the mantle similar to this has been submitted for publication by N. L. Carter and H. Avé Lallemant. We are indebted to these authors for use of their experimental data and wish to accord clear priority to them and to D. T. Griggs for the discovery of power law creep in olivine.

Experimental Creep Equation

Hot-creep experiments from which the equation is derived have been carried out in the hot-creep apparatus of D. T. Griggs (1967). Our specimens are cores of rock ¼ inch in diameter, surrounded by a graphite tube furnace and a solid confining medium. The cores are compressed axially at confining pressures up to 20 kbar but usually at 15 kbar. Carter and Avé Lallemant (1970) conducted their experiments at constant temperature and strain rates in the range of 10^{-4} to 10^{-7} sec^{-1}. The stress difference, $\sigma_1-\sigma_3$, at 5 percent strain, was used to determine the creep equation. The results from their dry experiments at temperatures from 1000° to 1200°C (Carter and Avé Lallemant, 1970) give the relation

$$\dot{\epsilon} = 1.2 \times 10^{10}\, \sigma^{4.8} \exp \frac{-Q_c}{RT} \qquad (1)$$

where $\sigma=\sigma_1-\sigma_3$, the stress difference in kbar; Q_c is the activation energy for creep; R is the universal gas constant; and T is the temperature in °K. The activation energy is 119 ± 16 kcal/mole.

Although we use a different technique to determine the dependence of strain rate on stress and the activation energy for creep, we obtain similar results. For a specimen deforming at a constant strain rate in creep at moderate stress and $T/T_m=0.5$ to 0.8, we assume an equation of the form,

$$\dot{\epsilon} = A\sigma^n \exp \frac{-Q_c}{RT}$$

The stress exponent may be determined as follows: If the strain is allowed to relax at a fixed temperature, the specimen strain, ϵ, as a function of stress at any time during the relaxation process, is given by the modulus, k, of the apparatus and specimen,

$$\frac{d\sigma}{d\epsilon} = -k$$

Therefore, the rate of stress relaxation is given by

$$\frac{d\sigma}{dt} = -kA\sigma^n \exp \frac{-Q_c}{RT}$$

The exponent, n, can be determined at successive stresses, σ and σ', along the relaxation path by

$$n = \frac{\log\left[\left(\frac{d\sigma}{dt}\right)\Big/\left(\frac{d\sigma}{dt}\right)'\right]}{\log\,(\sigma/\sigma')} \qquad (2)$$

provided that steady-state flow is achieved. A linear $d\sigma/dt$ versus σ relationship implies that the flow is in steady state. In Figure 1,

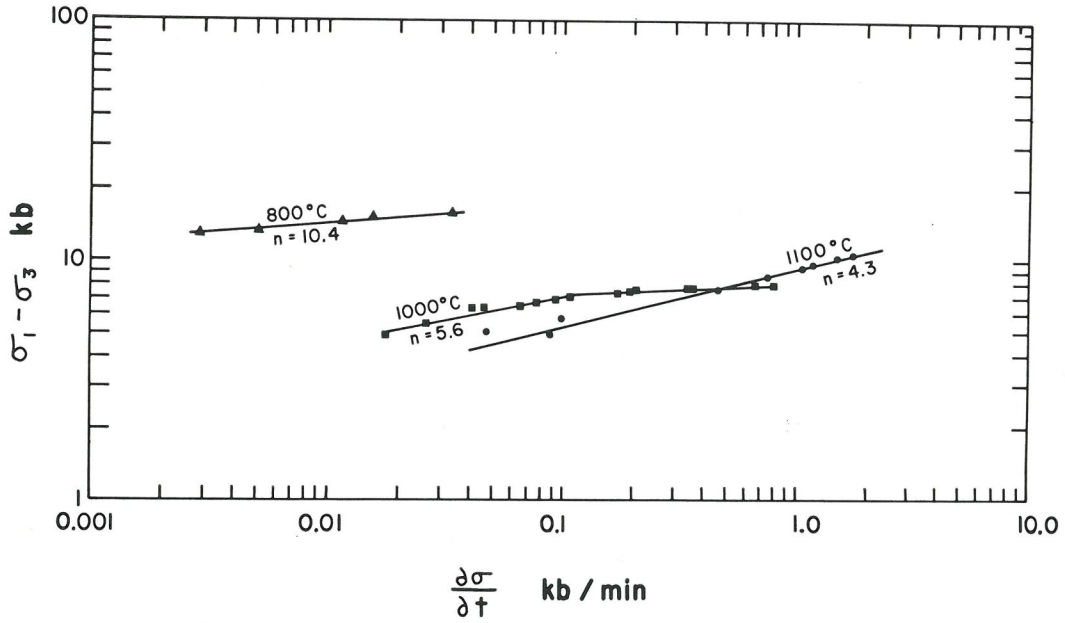

FIG. 1. Graph of stress difference, σ, vs rate of change of σ with time, $d\sigma/dt$. Data from stress-relaxation experiments at 800°, 1000°, and 1100°C on lherzolite at 15 kbar confining pressure.

σ is plotted against $d\sigma/dt$ for relaxation experiments at 15 kbar confining pressure and 800°, 1000°, and 1100°C for lherzolite specimens. The exponents are, respectively, 10.4, 5.6, and 4.3. The large decrease between 800° and 1000°C is related to a change in the creep process, which will be discussed in the latter part of this paper. The higher temperature values of n span the $n=4.8$ determination of Carter and Avé Lallemant (1970). The change in slope of the 1000°C experiment is probably due to a change in creep process as the strain rate decreased during the experiment.

Activation energies for creep can be determined by a method first used by Dorn and Sherby and their co-workers (Dorn, 1954). The steady-state creep rate immediately before and after a change in temperature from T_1 to T_2 is related to the activation energy for creep by

$$Q_c = \frac{T_2 T_1}{T_2 - T_1} \cdot R \cdot \left(\ln \frac{\dot{\epsilon}_2}{\epsilon_1}\right) \tag{3}$$

In experiments, the stress is held constant and the strain rate allowed to vary as the temperature is increased by small increments. This method is applicable, however, only over temperature ranges where the function, $f(\sigma)$, relating stress to strain rate is constant. Activation energies determined in this way in a dry, fine-grained artificial dunite vary rapidly over the range 850° to 950°C, but at 1000°C are about 100 kcal/mole.

We have conducted no systematic experiments in the presence of water. The results of Carter and Avé Lallemant (pers. commun.) from wet experiments differ considerably from those conducted dry and from the wet data of other investigators (R. L. Post, pers. commun.). There are considerable experimental difficulties in interpreting wet experiments because of uncertainties in the activity of water and in the magnitudes of the low-stress differences observed. In this paper, therefore, the mantle will be considered to be effectively dry.

On the basis of our experiments with lherzolite at 1000° and 1100°C and those by Carter and Avé Lallemant with Mt. Burnet dunite, the flow equation is given approximately by

$$\dot{\epsilon} = A\sigma^5 \exp \frac{-106}{RT \times 10^{-3}} \tag{4}$$

The uncertainty in the activation energy is probably ± 20 kcal/mole. Since Q_c was determined, in our experiments, at $T \leq 1000$°C and Q_c increased with temperature up to 1000°C, the value used is probably low. The constant, A, is 10^8 when σ is in kilobars.

THEORETICAL CREEP EQUATIONS

The models for creep processes in the mantle adopted by Weertman (1970) assume that vacancy diffusion is the rate-controlling process. The Herring-Nabarro theory assumes that at the highest temperatures and lowest stresses, diffusion of vacancies to and from grain boundaries is the rate-limiting process. This gives a strain rate, $\dot{\epsilon}$, proportional to stress, σ, at constant grain size,

$$\dot{\epsilon} = \left(\frac{\alpha D}{L^2}\right)\left(\frac{\sigma\Omega}{kT}\right) \tag{5}$$

where L is the grain diameter, α, a constant, Ω, the atomic volume, and k is Boltzmann's constant. The distribution of viscosities in the earth's mantle based on this model is also discussed by Gordon (1965) and McKenzie (1968), who has rederived Herring's (1950) original result.

Weertman (1968, 1970) shows that the strain rate due to vacancy diffusion between subgrain walls will not yield a viscosity independent of σ. Typically, the subgrain size in creep experiments is inversely proportional to stress and the creep rate is therefore dependent on stress to the third power, *i.e.*,

$$\dot{\epsilon} = \frac{\alpha D \sigma \Omega}{kT} \cdot \left(\frac{\sigma}{\mu L_0}\right)^2 \tag{6}$$

where the subgrain diameter, L, is

$$L = \left(\frac{\sigma}{\mu L_0}\right)^{-1} \tag{7}$$

where μ is the shear modulus and L_0 is a material constant.

Where dislocation climb is the rate-controlling process, Weertman (1968, 1970) predicts that creep rate is proportional to stress raised to the power n, where $n=4.5$ to 6. The experimentally determined dependence of creep rate on stress gives a similar result

in the temperature range (0.6 to 0.8) T_m. Because of this similarity, the experimental result, rather than the theoretical equation is used in our analysis of viscosity in the mantle.

The experimental determination of the activation energy for creep makes it possible to apply the theoretical creep laws to the mantle with a greater degree of confidence. As Weertman (1970) points out, pressure and temperature have the same effect on the creep rate as on the diffusion coefficient, D. The temperature effect on D is

$$D = D_0 \exp \frac{-Q_d}{RT} \tag{8}$$

where D_0 is a constant and Q_d, the activation energy for self-diffusion. If the rate-controlling process in creep is vacancy diffusion, then the activation energy for creep, Q_c, is the same as that for self-diffusion (Dorn, 1954; Sherby, *et al*, 1954; Sherby and Burke, 1968).

$$Q_c = Q_d \tag{9}$$

Weertman (1970) states that the effect of pressure on the diffusion coefficient is comparable to the effect of pressure on the melting temperature in °K, T_m. Sherby and Simnad (1961) found empirically that

$$D = D_0 \exp \left(\frac{-gT_m}{T}\right) \tag{10}$$

where g is a constant and T is the temperature in °K. Whether this relation holds at high confining pressure is unknown, but in the absence of experimental data on the effect of pressure on the creep rate, it will be used here to make our analysis consistent with Weertman's (1970). The value of g and D_0 can now be calculated from equations (8)–(10), given the activation energy, Q_c, and the assumption following Shewmon's (1963) rule that at T_m, $D = 10^{-8}\text{cm}^2\ \text{sec}^{-1}$. Thus, $g = 26.4$ and $D_0 = 10^{3.5}\text{cm}^2\ \text{sec}^{-1}$.

The effective viscosity ($\eta = \sigma/\dot{\epsilon}$) as a function of depth in the mantle can now be calculated from these flow equations when they have been modified to take into account the pressure effect on melting temperature. The experimental creep law can be restated as follows:

$$\dot{\epsilon} = 10^8 \exp \left(\frac{-26.4T_m}{T}\right) \sigma^5 \tag{11}$$

where σ is in kilobars and T_m is taken to be the solidus temperature for olivine, Fo_{90}. The variation of T_m with depth (hence, pressure), shown in Figure 2, is taken from Davis and England (1964) and assumed to be linear from 0 to 400 km. Below 400 km, a spinel phase will presumably take the place of olivine, but we have no experimental data for spinels. Qualitatively, however, with greater depth, the increase in effective viscosity shown by Gordon (1965) and Weertman (1970) is undoubtedly correct, provided the increase of T_m with depth exceeds the rate of increase of T.

The Herring-Nabarro creep equation,

$$\dot{\epsilon} = \frac{\alpha\sigma\Omega D_0 \exp \dfrac{-26.4T_m}{T}}{L^2kT} \tag{12}$$

can be evaluated, taking $\alpha = 5$ (Weertman, 1970) and $\Omega = 1.1 \times 10^{-23}$, and assuming an average grain diameter for the olivine of the mantle. The only data on grain size come from xenoliths of olivine-bearing ultramafic rocks of mantle origin brought up in volcanic eruptions. There is considerable variation within even a single suite of xenoliths, as shown in Figure 3. The smallest average grain size we have observed is about 1/2 mm in the lherzolite xenolith used for our experiments. Six specimens of dunite xenoliths from the 1801 flow from Hualalai (Jackson, 1968) have average grain diameters ranging from 1 mm to 1 cm. Grains as large as 10 cm occur in this flow and elsewhere. For the analysis to follow, we have taken $L = 1$ cm. It should be borne in mind that since the viscosity is proportional to L^2, an error of an order of magnitude in our assumption of grain size will result in an error in viscosity of two orders of magnitude. It should be noted also that there is no dependence of effective viscosity on L in the experimental flow equation or the subgrain vacancy diffusion model.

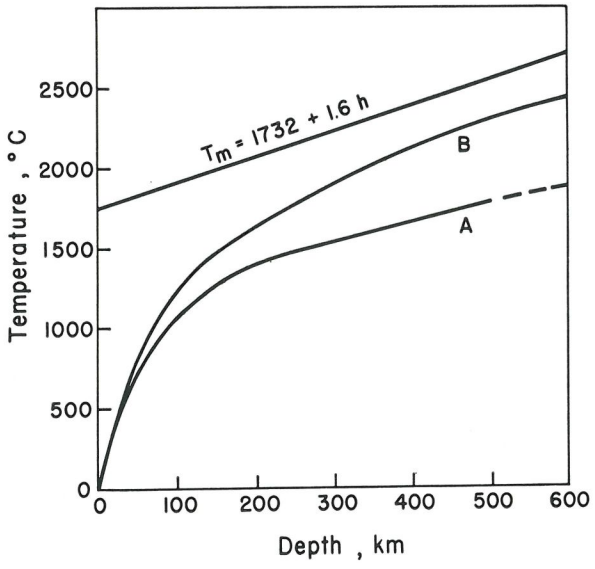

FIG. 2. Geothermal gradients for the upper mantle and the solidus temperature for olivine, Fo_{60}, (Davis and England, 1964) as a function of depth, h. Gradient A: Shield gradient of Clark and Ringwood (1964). Gradient B: Gradient for fractionated earth from thermal history calculations of Lee (1968).

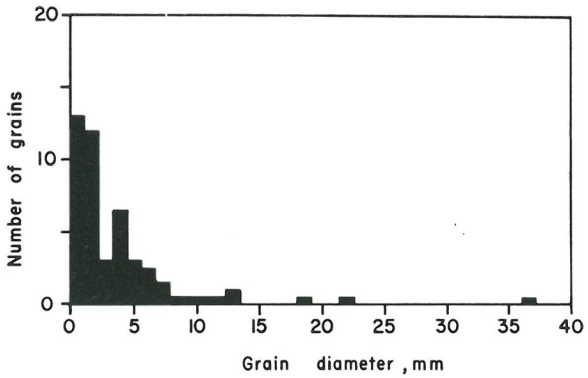

FIG. 3. Frequency of olivine grain diameters in lherzolite xenoliths from Lunar Crater, Nye County, Nevada.

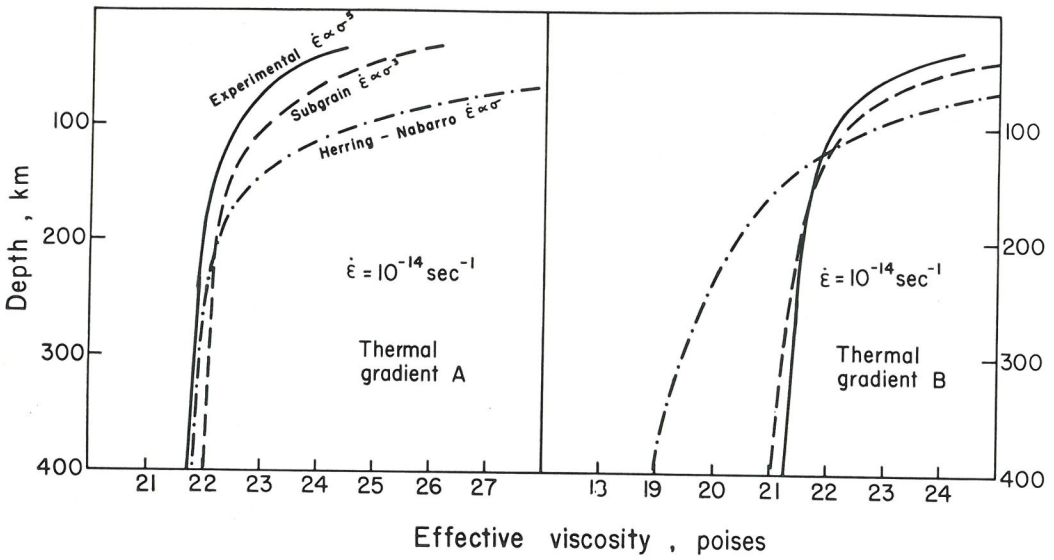

FIG. 4. Effective viscosity calculated for the upper mantle as a function of thermal gradient and the flow law. Strain rate is fixed at 10^{-14} sec^{-1}. Left: viscosity along shield thermal gradient of Clark and Ringwood (1944). Right: viscosity along gradient from Lee's (1968) thermal history calculations.

For Herring-Nabarro creep by diffusion between subgrain boundaries, Eq. (12) becomes

$$\dot{\epsilon} = \frac{\alpha\sigma^3\Omega D_0 \exp \dfrac{-26.4T_m}{T}}{kT(L_0\mu)^2}$$

The term $L_0\mu$ can be evaluated from measurements of olivine subgrain diameters in steady-state creep tests on lherzolite (see Eq. (7), Fig. 10). From the average of two experiments at 4.6 and 9.5 kbar differential stress, $L_0\mu = 2.4\times10^5$ dyne cm^{-1}.

A wide range of possibilities exists for geothermal gradients down to 400 km. We, therefore, have chosen two different models—one low (A, Fig. 2), one high (B)—from the literature and attach no special significance to them except as they show the effect of different temperature gradients on the viscosity.

The effective viscosity as a function of depth in the mantle for the three flow equations and temperature distributions A and B is shown in Figure 4. Because the viscosity is dependent on stress or on strain rate for the power law flow equations, an average strain rate of 10^{-14} sec^{-1} is assumed. We justify the use of this strain rate by pointing out that, given a sea-floor spreading velocity of 5 cm yr^{-1}, shearing beneath the plate is unlikely to be distributed over an average thickness of mantle less than 30 km or greater than 3000 km. As an order-of-magnitude estimate, therefore, $\dot{\epsilon} = 10^{-14}$ sec^{-1} is probably adequate. Of course, the strain rate may be much more rapid locally, as in the vicinity of faults or possibly in the source regions of volcanoes.

The principal feature of interest in Figure 4 is the dependence of the creep process on temperature distribution. If the shield temperature distribution of Clark and Ringwood (1964) (Curve A) is followed, below about 200 km, power law creep and Herring-Nabarro creep give approximately the same effective viscosity, about 5×10^{21} poise. Along the steeper thermal distribution (Curve B), Herring-Nabarro creep yields a much lower viscosity below about 130 km than does power law creep. In Figure 5, the effect of strain rate and stress on the creep process is shown at a temperature, $T = 3/4\ T_m$, corresponding to a depth of 150 to 250 km. At strain rates faster than 10^{-14} sec^{-1}, and stresses greater than about 100 bars, σ^5 creep dominates.

If temperature gradients are not abnormally high, deformation probably occurs by power law creep, at least in the upper 130 km of the mantle. Below that depth, uncertainty as to the thermal gradient and grain size in the mantle prevents any conclusion regarding the nature of the

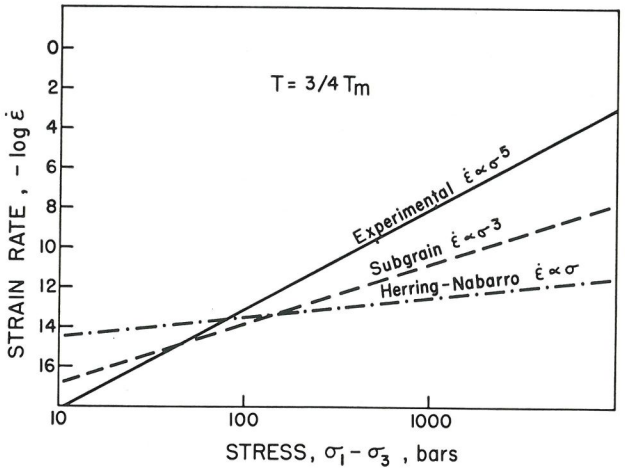

FIG. 5. Creep stress against strain rate, log $\dot{\epsilon}$, for different creep laws at $T = 3/4\ T_m$. The curves are derived from equations 11, 12, and 13.

creep law. Partial melting will drastically decrease the viscosity below that given by any of these models. In any case, it appears that the usual assumption of linear viscosity, at least for the uppermost mantle, can no longer be supported. This conclusion is supported by evidence from the internal structures in deformed peridotite xenoliths and alpine peridotites, given in the following section.

Mechanisms of Deformation

There is abundant evidence from creep of metals that the processes active in low-temperature creep at high stresses are quite different from those operating at intermediate stresses and temperatures (0.5 to 0.8 T_m) (Kennedy, 1963; Garofalo, 1965). Evidence of diffusion creep at high temperatures has been found for some metal oxides and polyvalent metals (McKenzie, 1968). It is generally held that the creep rate at low temperatures is dislocation-glide controlled and the rate at intermediate temperatures is dislocation-climb controlled. Typically, power-law creep in the intermediate temperature range is accompanied by the formation of subgrains. The subgrains are widely, though not universally, held to result from polygonization (Kennedy, 1963; Garofalo, 1965), a process in which dislocations climb from glide planes into planar walls. With increasing strain, the angle of tilt across such subgrain walls increases.

If creep is produced by sequential processes, such as glide of dislocations followed by climb, the slower process will be rate controlling. Creep in the power law region of stress and temperature, even though the rate-controlling process is climb, might therefore give rise to microstructures indicative of glide.

Where creep may take place by one or another of several nonsequential processes, the fastest of these will be rate controlling. At high temperature, where mass diffusion of vacancies between grain boundaries is the fastest process, other processes, such as glide, would be excluded. Creep deformation by mass diffusion of vacancies between grain or subgrain boundaries should result in inequant grains showing no internal relicts of deformation. This flattening of the grains might be erased by grain-boundary migration, thereby yielding equant individual crystals. Therefore, creep by vacancy diffusion between grain boundaries conceivably could leave no trace of the deformation.

The purpose of the next section is to compare the microstructures in the experimentally deformed olivines with those in the naturally deformed mineral. Where the two are the same, the creep processes, and hence the flow equations, should be the same. A considerable body of metallurgical data supports this conclusion.

Microstructural Effects—Slip

The glide mechanisms in experimentally deformed olivine are a function of temperature and strain rate (Raleigh, 1968). Carter and Avé Lallemant (1970) and our present work confirm the result reported earlier that glide in

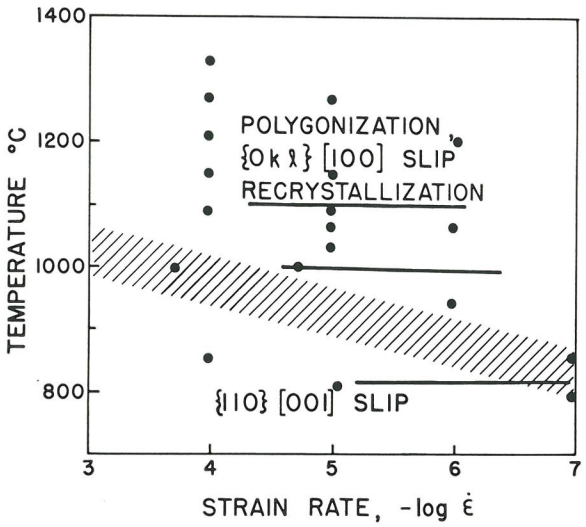

Fig. 6. Strain rates and temperatures, ●, for dry constant-strain-rate experiments on lherzolite at 15 kbar confining pressure. Hachured boundary between glide in the direction [001] and pencil glide in the direction [100] plus recrystallization and polygonization. Heavy solid lines indicate the $\dot{\epsilon}$ and T where relaxation tests were conducted. The 1000°C and 1100°C runs indicate $\dot{\epsilon} \propto \sigma^5$ approximately.

olivine occurs preferentially on {110} [001] at lower temperatures and higher strain rates, and on {0*kl*} [100] at higher temperature and lower strain rates. At even higher temperatures, greater than 0.7 T_m at laboratory strain rates, Carter and Avé Lallemant (1970) find that glide in [100] occurs preferentially on (010).

Specimens of lherzolite deformed at 15 kbar confining pressure at the temperatures and strain rates shown in Figure 6 were examined to determine the slip mechanism in olivine. The techniques used have been described previously (Raleigh, 1968) and include measurement with a universal stage microscope of the lattice rotations associated with kinking and of the orientations of deformation lamellae. At temperatures above the hachured region in Figure 6, slip is concentrated on planes in the [100] zone, and kink bands form nearly parallel to (100). Toward the higher temperatures, as shown in Figure 7, the slip planes, determined from external rotations across the (100) kink-band boundaries, are oriented preferentially on (010) and {032} or other planes near {032} .

The region of temperature and strain rate in which both the activation energy determination and the relaxation experiments leading to creep equation (3) were conducted is between 1000° and 1200°C and strain rates of 7×10^{-5} to 7×10^{-7}/sec. The predominant glide mechanism for olivine in this region is {0*kl*} [100]. Determinations of the slip mechanism in the naturally deformed suites of peridotites indicate that {0*kl*} [100] glide also predominates in these olivines.

Four suites of periodotites were examined: (1) highly strained lherzolite xenoliths from the Lunar Crater area in

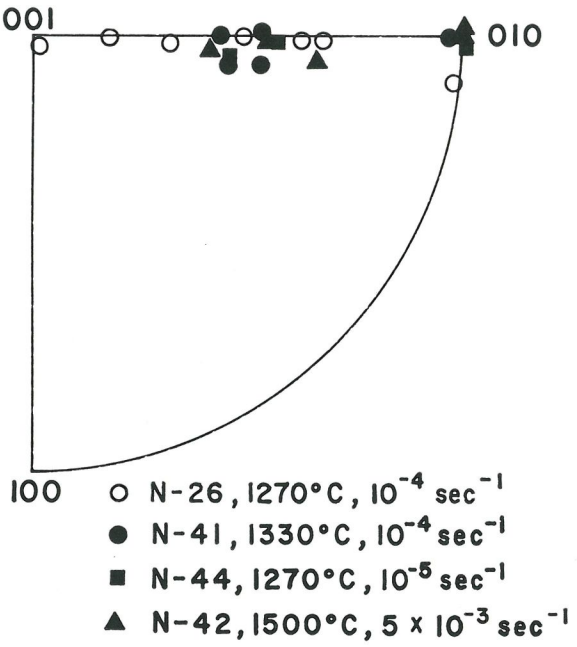

FIG. 7. Poles to slip planes in [100] as determined from external rotations across kink band boundaries in experimental specimens.

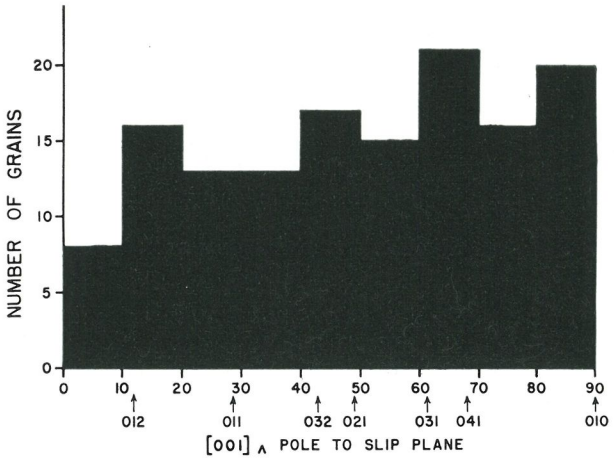

FIG. 9. Frequency of slip planes on $\{0kl\}$ versus angle between pole to slip plane and [001].

Nye County, Nevada (loaned to us by Newell Trask); (2) dunite xenoliths from the 1801 flow from Hualalai on Hawaii (source: E. D. Jackson)—the olivines in these are less deformed than the Lunar Crater specimens; (3) alpine peridotite from Cypress Island, Washington (Raleigh, 1965); and (4) dunite from the outcrop of ultramafic rock at Union Bay, Alaska (Ruckmick and Noble, 1959). Kink banding on {100} is the principal evidence of plastic strain in olivine in all of these specimens. Measurement of lattice rotations across kink band boundaries (Raleigh, 1968) in a large number of grains shows that slip of the system $\{0kl\}$ [100] is without exception the predominant mechanism of glide (Fig. 8). There is only a slight tendency for the glide planes to cluster around (010) in preference to other $\{0kl\}$ planes (Fig. 9).

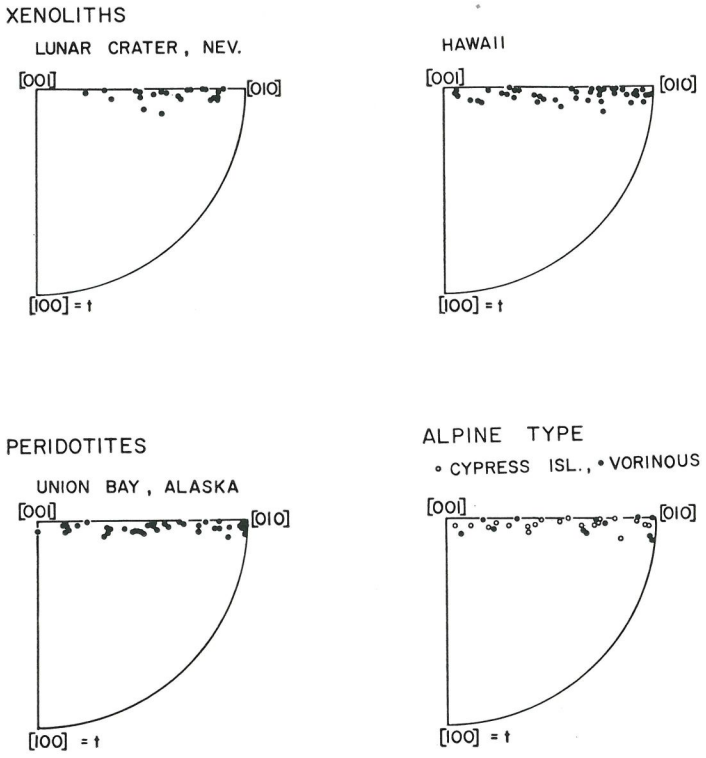

FIG. 8. Poles to slip planes in [100] in naturally deformed peridotites. Determined from external rotations across (100) kink bands.

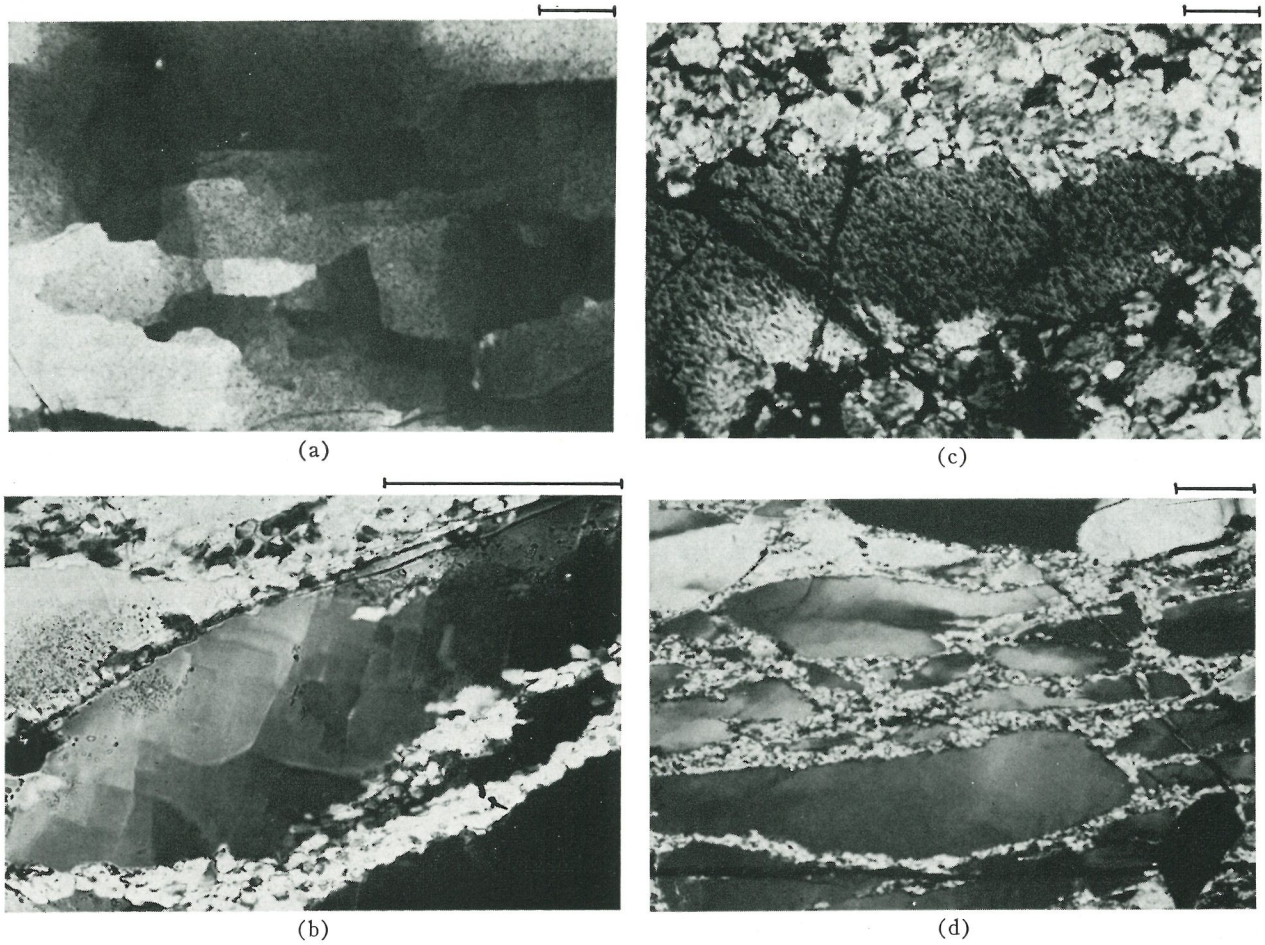

FIG. 10. Microstructural features in olivine. Transmitted light, crossed polarizers. Bar scale length = 100 microns. a. Olivine subgrains in a nodule from Lunar Crater, Nye County, Nevada, Specimen No. LC 11-1. b. Olivine subgrains in N-26, an experimentally deformed lherzolite. $T = 1270°C$, $\dot{\epsilon} = 1.07 + 10^{-4}$ sec $^{-1}$. c. Grain boundary recrystallization in a Lunar Crater nodule, Specimen No. LC-127. d. Grain boundary recrystallization in an experimentally deformed lherzolite, N-27. $T = 1150°C$, $\dot{\epsilon} = 1.07 \times 10^{-1}$ sec^{-1}.

Recrystallation along grain boundaries is common at temperatures above 1000°C and strains greater than 5 to 10 percent as shown in Figure 10, c, d. The textural resemblance of the experimentally and naturally deformed materials is marked.

SUBGRAINS

When olivine-bearing rocks are deformed at temperatures about 100° higher than those at which $\{0kl\}$ [100] glide begins, deformed olivines contain small, clearly defined polygonal subgrains (Fig. 10b). The subgrains tend to be rectangular with boundaries approximately parallel to (100) and (001). The boundaries lie between olivines of slightly differing lattice orientations and, in transmitted light, are apparent only between crossed polarizers. The tilts across the boundaries are small, generally less than 5°. Observations of subgrains are therefore difficult to make unless strains are sufficiently large so that tilts are great enough to render the orientation differences discernible.

Subgrains are found in both suites of basaltic xenolith examined. In the Hawaiian xenoliths, the dunites of the 1801 flow from Hualalai best display the structure. The morphology and crystallographic orientation are similar to the experimentally produced subgrains. In both the Lunar Crater and Hawaiian specimens, the subgrain dimensions are about ten times the size of those produced in experiments (Fig. 10a).

The diameters of subgrains in creep experiments on metals are inversely proportional to the creep stress (Garofalo, 1965; Jonas, *et al.* 1969; Sherby and Burke, 1968). Weertman (1970) gives L, the subgrain diameter, as

$$L = \left(\frac{\sigma}{\mu L_0}\right)^{-1} \tag{7}$$

where L_0 is a constant and μ the rigidity. Measurements of subgrain diameters parallel to [001] and [100] in the experimentally and naturally deformed olivines are plotted in Figure 9; values of μ were calculated from data reported by Anderson *et al.* (1968). The dimension along [100] is about 0.6 of that along [001] in the four sets of measurements. Figure 11 shows the range of measurements in the

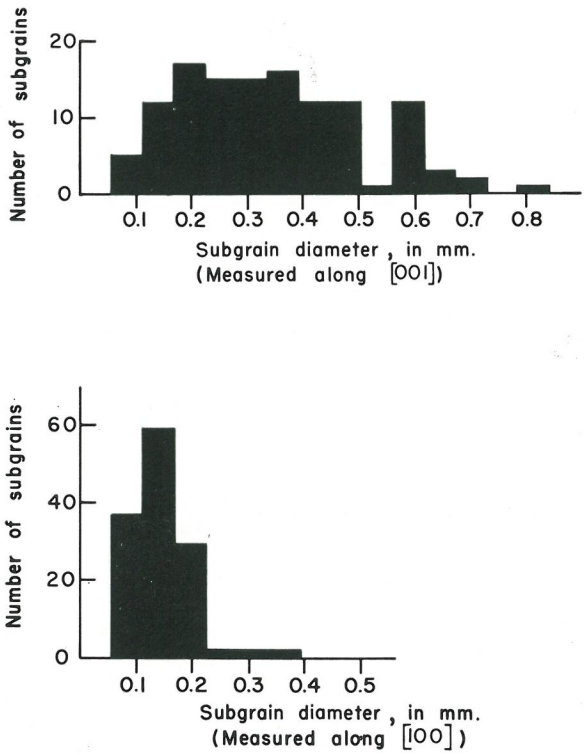

FIG. 11. Frequency of subgrains having diameters measured along [001] and [100]. Lunar Crater, Nevada, lherzolite xenoliths.

Lunar Crater specimens and illustrates the differences between the two dimensions as well as the variability in the measurements. The variability is greatest along [001]. In the two experimental specimens, N-26 and N-41, in which a large number of measurements were possible, the relation, Eq. (7), holds fairly well. Plotting the measurements from naturally deformed xenoliths from Lunar Crater and Hawaii in Figure 12 gives, in both cases, differential stresses of approximately 1 kbar, provided μ does not change significantly between the natural and experimental conditions.

Because too few measurements have been made on experimental specimens, and these few in such a small range of stresses, the results in Figure 9 are not of great quantitative significance. As more data become available to provide an adequate test, this promising method will, we hope, enable us to make quantitative estimates of the magnitude of stresses in the crust and mantle.

DISCUSSION

The similarity of microstructures formed in the five-power-law region in the experimentally deformed specimens to those found naturally in xenoliths is striking. Pencil glide on the system $\{0kl\}$ [100] gives way to other mechanisms at temperatures higher and lower than those at which the experimental creep equation was determined. Yet, in the suites of naturally deformed specimens examined, pencil glide is clearly the predominant glide mechanism. The morphology and boundary orientations of subgrains in specimens deformed experimentally by creep in the five-power-law region are similar to those of naturally deformed xenoliths, additional evidence that creep in the upper mantle follows an equation similar to the one determined experimentally.

Water could, of course, alter the parameters of the creep equation from the dry case without having a large effect on the microstructures. Since it is probable that at least small quantitites of water are present in the mantle, its effect raises a difficulty which, unfortunately, we have been unable to assess.

By extrapolating the experimental creep equation given here and the theoretical equations for Herring-Nabarro creep to conditions in the mantle, it appears that for a region from about 200 to 400 km or deeper, the effective mantle viscosity will be no greater than about 10^{22} poise. Over at least the upper 130 km, the experimental power law gives lower effective viscosities at strain rates compatible with sea-floor spreading. Below 130 km or so, depending strongly on the thermal gradient, either Herring-Nabarro creep or the experimental creep law may hold. For stresses below about 100 bars or strain rates below 10^{-14} sec^{-1}, at temperatures around 1300°C, the viscosity for the Herring-Nabarro model will be less than for power law flow.

The comparison between microstructures produced experimentally in power-law creep and those occurring nat-

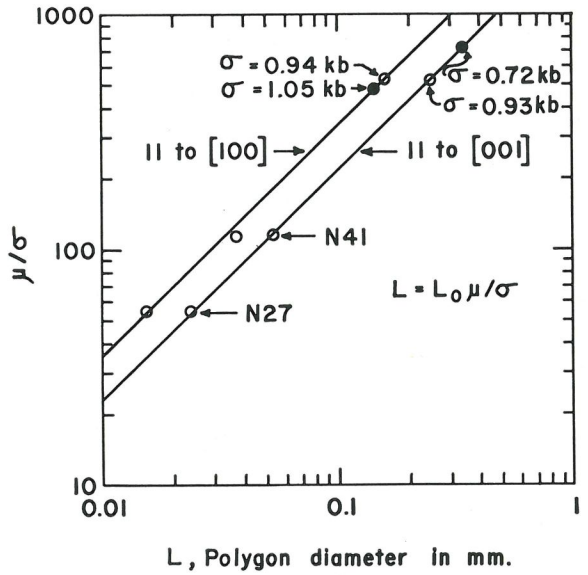

FIG. 12. Plot of log subgrain diameter, L, versus μ/σ where linear extrapolation according to $L = L_0\ \mu/\sigma$ assumed. N-26, N-41 experimental subgrains at stresses of 9.5 and 4.6 kbar, respectively. Stresses for subgrain diameters of naturally deformed olivine in xenoliths calculated.

urally in xenoliths within basalts indicates that power-law creep has taken place within the mantle. Whether this evidence is relevant to the flow process over large regions of the mantle is not clear. In any case, the depths from which such xenoliths might reasonably originate are within the range predicted for the experimental power law equation. Further work on the subgrain diameters may make it possible to estimate the magnitude of the creep stresses at which such mantle-derived rocks were deformed.

Acknowledgments

Ruth Dale Stevens made most of the universal stage measurements on the naturally deformed olivines. Newell Trask and E. D. Jackson of the U.S. Geological Survey kindly loaned us the suites of deformed xenoliths.

References

Anderson, O. L., E. Schreiber, R. C. Liebermann, and N. Soga (1968) Some elastic constant data relevant to geophysics. *Rev. Geophys.* **6,** 491–523.

Carter, Neville, and Hans Avé Lallemant (1970) High temperature flow of dunite and peridotite, *Bull. Geol. Soc. Amer.* (in press.)

Clark, S. P., Jr., and A. E. Ringwood (1964) The density distribution and constitution of the mantle. *Rev. Geophys.* **2,** 35–88.

Davis, B. T. C., and J. L. England (1964) The melting of forsterite up to 50 kilobars. *J. Geophys. Res.* **69,** 1113–1116.

Dorn, John E. (1954) Some fundamental experiments on high temperature creep. *J. Mech. Phys. Solids.* **3,** 85–116.

Garofalo, Frank (1965) *Fundamentals of Creep and Creep-Rupture in Metals.* Macmillan Company, New York.

Gordon, Robert B. (1965) Diffusion creep in the earth's mantle. *J. Geophys. Res.* **70,** 2413–2418. .

——— (1967) Thermally activated processes in the earth: Creep and seismic attenuation. *Geophys. J. Roy. Astron. Soc.* **14,** 33–43.

Griggs, D. T. (1967) Hydrolytic weakening of quartz and other silicates. *Geophys. J. R. Astr. Soc.* **14,** 19–31.

Herring, C. (1950) Diffusional viscosity of a polycrystalline solid. *J. Appl. Phys.* **21,** 437–445.

Jackson, E. D. (1968) Character of the lower crust and upper mantle beneath the Hawaiian Islands. *Abstr., 23 Int. Geol. Cong.,* 23.

Jonas, J., C. M. Sellars, and W. J. McG. Tegart (1969) Strength and structure under hot working conditions. *Met. Rev.* **130,** 1–24.

Kennedy, A. J. (1963) *Process of Creep and Fatigue in Metals,* John Wiley and Sons, New York.

Lee, W. H. K. (1968) Effects of selective fusion on the thermal history of the earth's mantle. *Earth Planet. Sci. Lett.* **4,** 270–276.

McKenzie, D. P. (1968) The geophysical importance of high-temperature creep, *In* R. A. Phinney, Ed., *The History of the Earth's Crust,* Princeton Univ. Press, Princeton, N.S.

Raleigh, C. B. (1965) Structure and petrology of an alpine peridotite on Cypress Island, Washington, U.S.A., *Beit. Mineral. Petrog.* **11,** 719–741.

——— (1968) Mechanisms of plastic deformation of olivine. *J. Geophys. Res.* **73,** 5391–5406.

Ruckmick, J. C., and J. A. Noble (1959) Origin of the ultramafic complex at Union Bay, southeastern Alaska. *Geol. Soc. Amer. Bull.* **70,** 981–1017.

Sherby, O. D., R. L. Orr, and J. E. Dorn (1954) Creep correlations of metals at elevated temperatures. *J. Metals.* **6,** 71–80.

———, and M. T. Simnad (1961) Prediction of atomic mobility in metallic systems. *Trans. Amer. Soc. Metals.* **54** 227–240.

———, and P. M. Burke (1968) Mechanical behavior of crystalline solids at elevated temperatures. *Prog. Mater. Sci.* **13,** 325–329.

Shewmon, P. G. (1963) *Diffusion in Solids.* McGraw-Hill, New York.

Weetman, J. (1968) Dislocation climb theory of steady-state creep. *Trans. Amer. Soc. Metals.* **61** 681–697.

——— (1970) The creep strength of the earth's mantle. *Rev. Geophys.* (in press).